

5th Symposium on
Flow Visualization
Prague, 1989

Published in Flow Visualization V: Proc. of the 5th International Symposium,
organized by the International Flow Visualization Society
Prague August 1989, copyright CRC Press 1990, ISBN 0-89116-887-7
DOI of this article: 10.5281/zenodo.14004

Automatic Particle Tracking Velocimetry beneath a wind-stressed wavy water surface with image processing

Dietmar Wierzimok
*Institute for Environmental Physics,
University of Heidelberg, Im Neuenheimer Feld 366
D-6900 Heidelberg, West Germany*

Bernd Jähne
*Scripps Institution of Oceanography
La Jolla, CA 92093-0212, USA*

Abstract

The turbulent flow in water close to the wavy wind-stressed water surface has been measured in a large circular wind-water tunnel with a low cost image processing system, using a CCD camera. The flow field beneath the moving air-water interface is being visualized by small particles illuminated by a thin light sheet. The velocity vectors have been determined by image sequence analysis of up to 32 binary images. Since every particle is traced along its full path within the light sheet, both the Eulerian and the Lagrangian velocity fields can be calculated. Simultaneously, the wave profile is determined.

particle tracking; image sequence processing; water surface; flow field; wind-water tunnel;

1 Introduction

Wind-driven turbulent flow close to a free water surface has attracted more attention recently, because of its importance for transfer processes across a air-water interface. The exchange of gases between air and water is a ubiquitous phenomenon. It controls reaeration of rivers and lakes and determines the global flux of climate relevant trace gases such as CO₂ and methane between the atmosphere and the ocean /1/. Knowledge of the of air-sea gas exchange mechanisms and of the turbulence structure close

to the wave region of a free-surface water flow is very limited.

Experimentally, there are two principle ways to gain to this layer. First, a probe mounted on a wave follower can be used. The state-of-the-art instrumentation is a laser doppler anemometer using a scanning mirror to follow the waves /2/. Yet interpretation of point measurements close to a moving surface is difficult. Secondly, methods based on flow visualization offer the advantage of extended area measurements including the region up to the water surface. Different techniques have been applied to make the flow field visible. For a quantitative determination of the velocity field, particle tracking techniques are most suitable. The main problem here is the fast and quantitative derivation of the velocity data from the images /3,4/. Recently, digital image processing techniques have been used to evaluate particle tracking images /5,6,7/. This paper describes a particle tracking technique suitable to study the turbulent water flow close to the water surface. The advantage of using image sequences instead of images pairs for the determination of the velocity field are pointed out.

2 Experimental set up

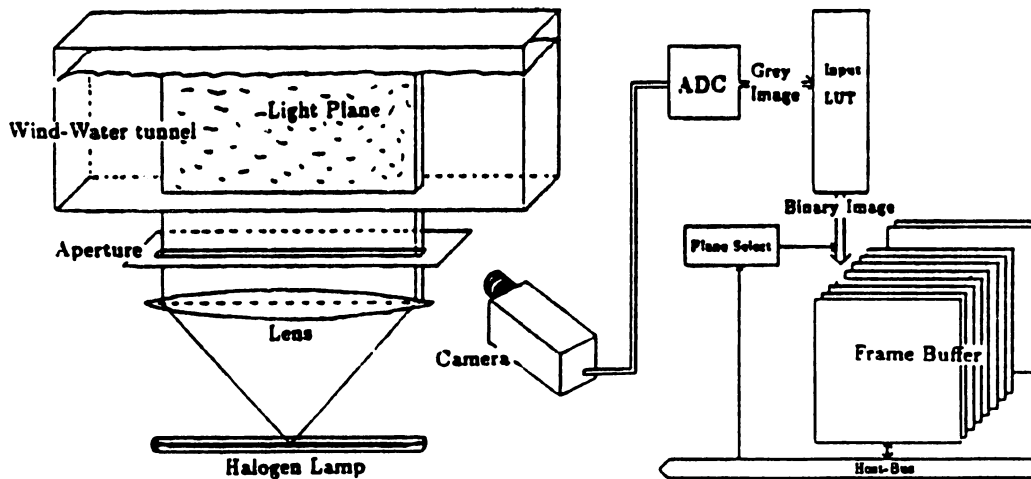


Figure 1 Arrangement of the wind-water tunnel, the optical system and the image processing system.

The experiments have been performed in the large circular wind-water tunnel at the Institute of Environmental Physics, Heidelberg University. The annular water channel of the facility has an outer diameter of 4 m and a width of 0.3 m. The maximum water depth is 0.3 m. In the walls, bottom and ceiling the tunnel is equipped with several glass windows for optical instruments. The turbulent flow has been made visible by spherical Latex-particles (polystyrol) with sizes ranging from 50-150 μm . Because their density is close to water (1.05 g/cm^3) they show only low bouyancy effects and can be used over a long time /8/. The particles are illuminated from below by a vertical light plane, generated by a linear halogen lamp and an optical projection system (figure 1). The plane is oriented parallelly to the mean tunnel flow. The particles in the 1.5 cm thick light sheet are observed perpendicularly to it with a CCD-video camera. The lens had a focal length of 25 mm and an aperture of 0.95.

Because of the continuous illumination the exposure time is 40 ms. Consequently, the moving particles appear as thin streak lines in the images.

The video data are digitized and stored as binary images in the frame buffer of two different PC-based image processing systems, a MVP-AT (Matrox, Canada) and a FG-100 (Imaging Technology, USA). Both systems digitize video image data with 256 grey values (8 bit) and a spatial resolution of 512×512 pixels and can store up to four such images in the frame buffer. As host an HP/RS20, an IBM compatible PC with an Intel 386 processor is used. Image sequences have been digitized at different wind speeds ranging from 0.5 m/s to 6.4 m/s and with wave amplitudes (trough to crest) up to 6 cm. The observed area was 9 cm high and 13.5 cm wide. It included the water surface.

3 Image Processing

In the following consecutive sections the steps from digitizing the image sequences up to the calculation of the velocity vectors are described.

Real-Time Segmentation

Image sequences consume large volumes of memory. A sequence of only one second duration (25 images) needs 6 Mbytes of frame buffer. To overcome this problem a real-time segmentation has been implemented with the input look-up table (IN-LUT) of the image processing system. The global threshold of the IN-LUT was set instructively. The digitized video data pass the IN-LUT and are stored as binary images in subsequent bit planes of the frame buffer. In this way up to 32 consecutive images of a sequence can be stored in a 1 Mbyte frame buffer.

The time difference between two following images can be set in multiples of 40 ms. With slow particle motions 12.5 images/sec have been used, in the other cases 25 images/sec. Figures 8 and 9 show two typical sequences. Each contains 8 consecutive binary images in one image, where the particle traces from each image are coded with a different grey value.

Determination of the Wave Profile

The images (figure 8 and 9) also include the water surface as a thick wavy line in the upper part. On the one hand, this offers the advantage that the wave profile and the flow field can be determined simultaneously. This is an essential feature of the new technique since it allows a direct correlation of the wave and flow data. On the other hand, processing of the particle streaks is made more difficult. For a proper determination of the flow field the wave profile should contain only particle streaks. Thus the image features belonging to the wave profile must be removed.

The determination of the wave profile and its segmentation from the streak lines can be achieved with morphological operations. An *opening*-operation O /9/ is used to eliminate the particle traces in the binary images. The *opening*-operator works like a sieve, throwing away any object smaller than its grid size. The opening operation consists of an *erosion* operation followed by a *dilation* operation:

$$O f = D \mathcal{E} f$$

where \mathcal{E} and D are the *erosion* and *dilation*-operators, which can be written for binary

images as:

$$\mathcal{E}f(x, y) = \begin{cases} 1 & : f(x-i, y-j) \text{ AND } h(i, j) = 1 \quad \forall i \in [-\frac{n}{2}, \frac{n}{2}], j \in [-\frac{m}{2}, \frac{m}{2}] \\ 0 & : \text{else} \end{cases}$$

$$\mathcal{D}f(x, y) = \begin{cases} 1 & : f(x-i, y-j) \text{ OR } h(i, j) = 1 \quad \forall i \in [-\frac{n}{2}, \frac{n}{2}], j \in [-\frac{m}{2}, \frac{m}{2}] \\ 0 & : \text{else} \end{cases}$$

Each operation is performed with a binary $n \times m$ filter mask h consisting of ones alone. With this filter all closed objects smaller than n in x - and m in y -direction disappear. The whole processing takes about 60 s for a sequence of 32 images when the morphological operations are separated in line and column operations to reduce the computational costs. With a simple line thinning algorithm, at least an additional *erosion*-operation, the wave line can be reduced to its center line in each half frame for further processing. An image containing only particle streaks is obtained by subtracting the *opened* image from the the original image. The result of both operations is shown in figures 10 and 11.

Particle Tracking

Searching for the corresponding particle in the following image with a standard correlation method is not suitable for streak-line images, because of the very similar form and direction of neighbored particles, particularly in the more laminar areas of a flow field. However, a single streak-line image contains a first estimate of the particle velocity including the flow direction. This knowledge will be used to find the corresponding trace in the next image. The estimate of the particle velocity from one image is made simple by the interlaced norm of the video images. Odd and even lines of an video image are exposed with a time delay of $\delta t = 20$ ms. As a result, a trace of any object, moving with several pixels within 40 ms looks like shown in figure 2. The estimated velocity vector \tilde{v} of a moving particle is given by the difference between the center of gravity of pixels of the streak lines belonging either to the even \bar{x}_e or odd \bar{x}_o positions:

$$\tilde{v} = \frac{\bar{x}_e - \bar{x}_o}{\delta t}$$

The interlaced structure is also important for segmenting moving particles from non-moving line structures. They always give a zero displacement vector \tilde{v} .

Vector calculation

For correspondence analysis the estimated vectors are now prolonged from the equivalent position in the next image in steps of 0.2 (arbitrarily fixed) up to a defined maximal factor as long as a streak line is found. The velocity vector $v(x, y, t)$ for a particle is given by the difference vector between the centers of gravity, \bar{x} , of both streaks and the time difference between both images as

$$v(x, y, t) = \frac{\bar{x}_{t+\Delta t} - \bar{x}_t}{\Delta t}$$

The particle is accepted in the next image when the deviation of \tilde{v} in both images (\tilde{v}_1 and \tilde{v}_2) is within the limit a given by

$$a > \|\tilde{v}_1 - \tilde{v}_2\|$$

The limit a represents the maximal accepted acceleration. In this way a particle is tracked through the whole image sequence, or until its trace is lost.

Spatial calibration

The real (world) coordinates of the calculated velocity have been obtained by a calibration measurement. A grid with a mesh width of 0.5 cm has been positioned at the center of the light sheet. If we neglect the depth of the light sheet, the transformation of the world coordinates $P(x, y)$ (9 cm \times 13.5 cm) to the image coordinates $P(x', y')$ (512 \times 512 pixels) are given as a central projection from one plane onto the other as

$$x' = \frac{a_1x + a_2y + a_3}{c_1x + c_2y + 1} \quad \text{and} \quad y' = \frac{b_1x + b_2y + b_3}{c_1x + c_2y + 1}$$

With the $i > 4$ pass points P_i , an overdetermined set of $2i$ linear equations is given for the eight projection parameters $a_1 \dots c_2$ which has been solved with standard techniques /10/. In the simple case of parallel planes and no rotation between the two coordinate systems, the x and y coordinates are independent and the coefficients a_2 , b_1 , c_1 and c_2 become zero. The remaining coefficients a_1 , a_3 , b_2 and b_3 can be calculated from only two pass points. An accuracy of about 0.3% in both directions could be achieved.

4 Results

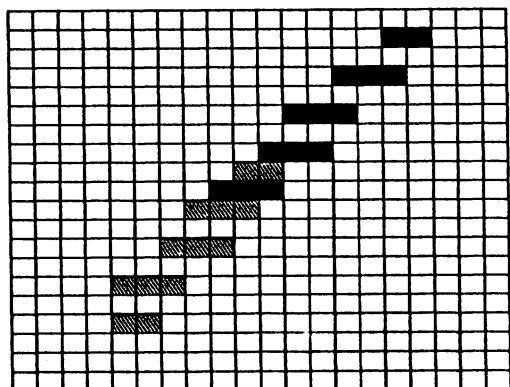


Figure 2 Typical interlaced structure of a moving particle digitized from a video signal.

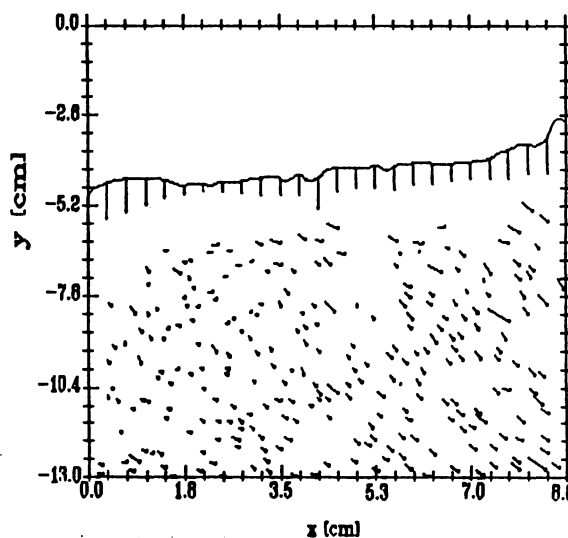


Figure 3 Calculated velocity vectors from image 21 to 22 of the sequence in figure 8 ($v_w = 6.2$ m/s). Additionally the water surface and its vertical velocity is plotted.

In figure 8 and 9 two typical scenes with wind speed of 6.2 m/s and 2.9 m/s, respectively, are presented including 8 consecutive images of the sequence. The particle traces of each image are denoted by a different grey value. Figure 10 and 11 show the segmentation of the scene from figure 8 into two images. One contains the wave, the other the particle motions. Two consecutive images from the sequence in figure 8 were used to determine the Eulerian streamlines (figure 3) simultaneously with the wave profile and horizontal velocity of the water surface. From the whole sequence 4746 vectors within 782 trajectories have been calculated within 5 minutes. Distributions

of the horizontal and vertical velocities, v_x and v_y , from all vectors of the sequence are shown in figure 4, while figure 5 presents a typical distribution of v_y as a function of the water depth y . The phase information of the wave amplitude at the middle of every image allowed an estimation of the correlation between wave and velocity field, (figure 6). Finally, Lagrangian streak lines are presented for a scene with less particles calculated from a sequence of 16 images (figure 7).

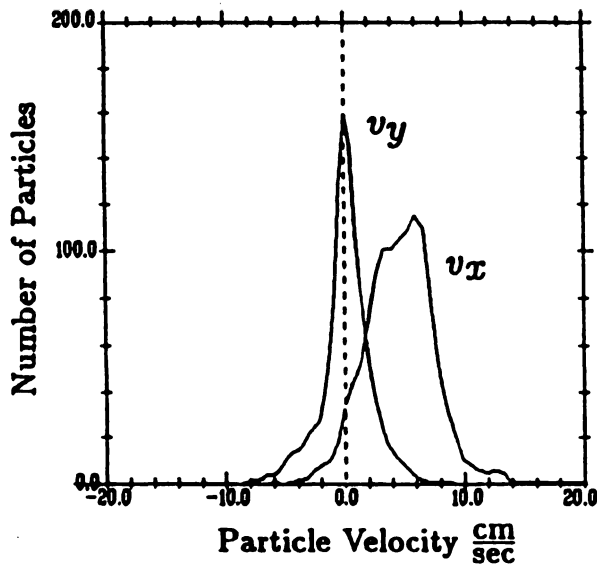


Figure 4 Distribution of velocity components v_x and v_y of the scene from figure 3.

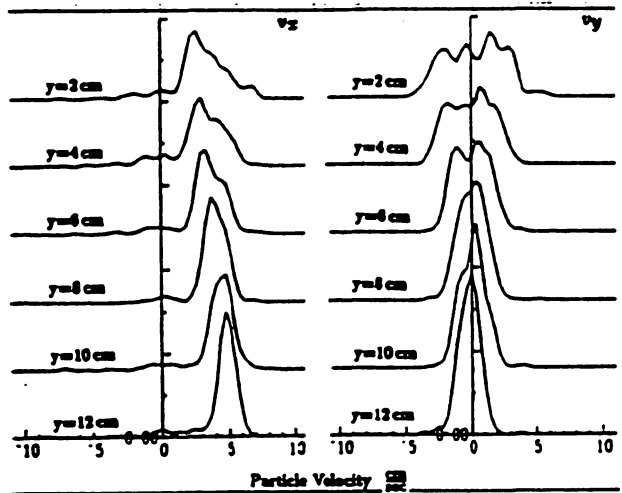


Figure 5 Typical distribution of v_y and v_x versus water depth.

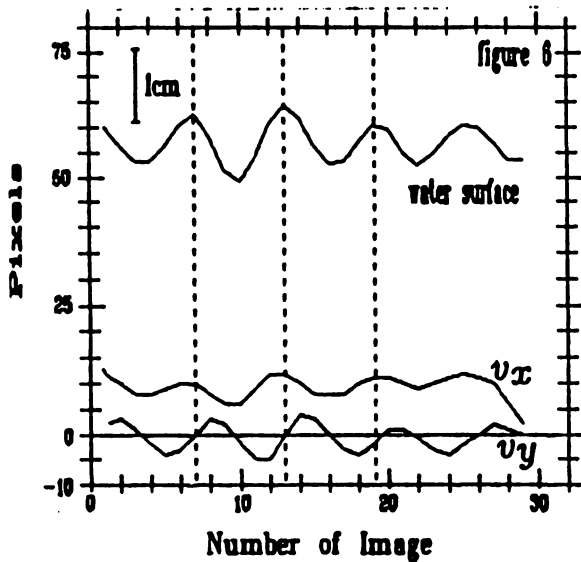


Figure 6 Qualitative demonstration of the temporal correlation between water surface and particle velocity. The time period of the sequence is 2.6 sec, the wind speed 4 m/s.

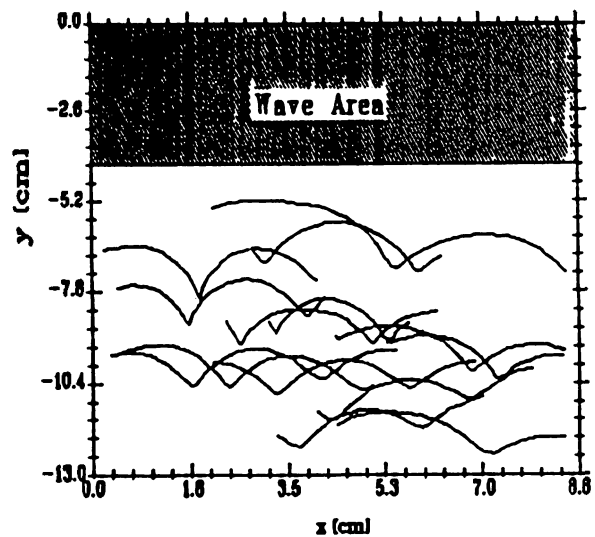


Figure 7 Lagrangian presentation of a scene with 139 detected particles. Only 15 trajectories, larger than 20 images are plotted.

5 Concluding Remarks

In this paper we have presented a versatile technique of particle tracking velocimetry for extended area velocity measurements beneath a moving water surface with an simultaneous estimation of wave parameters by picture processing. The first results are encouraging. The next steps aim at an improvement of the accuracy of the velocity into the subpixel range by the use of grey value instead of binary image sequences. Yet more important is an expansion of this technique to 3D-velocity measurements. One promising proposition is the use of stereo images.

References

- /1/ B. Jähne, K. O. Münnich, R. Bössinger, A. Dutzi, W. Huber, P. Libner: On the parameters influencing air-water gas exchange *J. Geoph. Res.*, 92, pp. 1937-1949, 1987
- /2/ T. K. Cheung and R. L. Street: Wave following measurements in the water beneath an air-water interface *J. Geoph. Res.*, 93, pp. 14,089-14,097, 1988
- /3a/ K. Okuda, S. Kwai, Y. Toba: Detailed observation of the wind surface flow by use of flow visualization *J. Oceanogr. Soc. Japan*, 32, pp. 53-64, 1976
- /3b/ K. Okuda: Internal flow structure of short wind waves, Part I. On the internal vorticity structure *J. Oceanogr. Soc. Japan*, 38, pp. 28-42, 1982
- /3c/ K. Okuda: Internal flow structure of short wind waves, Part II. The streamline patterns *J. Oceanogr. Soc. Japan*, 38, pp. 313-322, 1982
- /4/ A. A. Adamczyk, L. Rimai: 2-Dimensional particle tracking velocimetry (PTV): Technique and image processing algorithms, *Experiments in Fluids* 6, pp. 373-380, 1988
- /5/ Juan C. Agüí, J. Jiménez: On the performance of particle tracking *J. Fluid Mech.*, 185, pp. 447-468, 1987
- /6/ T. D. Dickey, B. Hartman, E. Hurst, S. Isenogle: Measurement of fluid flow using streak photography, *Am. J. Phys.* 52(9), 1984
- /7/ E. Maier: Die Vermessung von Strömungsfeldern mit Methoden der Bildverarbeitung, *Studienarbeit am Inst. f. Strömungslehre und Strömungsmaschinen, Universität Karlsruhe* 1986
- /8/ H.-E. Albrecht: *Laser-Doppler-Strömungsmessung*; Reihe: Physical research; Akademie Verlag Berlin, 1986
- /9/ J. Serra: *Image analysis and mathematical morphology*, Academic Press London, 1982
- /10/ S. A. Teukolsky, W. T. Vetterling: *Numerical recipes, the art of scientific computing*, Cambridge University Press, 1988.

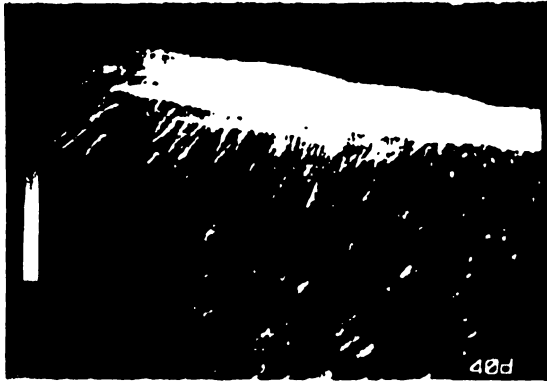


Figure 8,9,10 The 3 photos show the same particle streak sequence with a windspeed of 6.2 m/s and a mean flow velocity of 8 cm/sec , including each 8 consecutive images of the sequence. The particle traces of each binary image are denoted by a different grey value. Figure 9 shows the unprocessed scene, including both, wave and streak line, which are separated in figure 10 and 11 by morphological operators. In this sequence 4746 vectors for 782 particles have been calculated.



Figure 11 Particle streak sequence at a lower windspeed (2.9 m/s), and a mean flow velocity of 6 cm/sec (1318 detected particles, 14359 vectors).

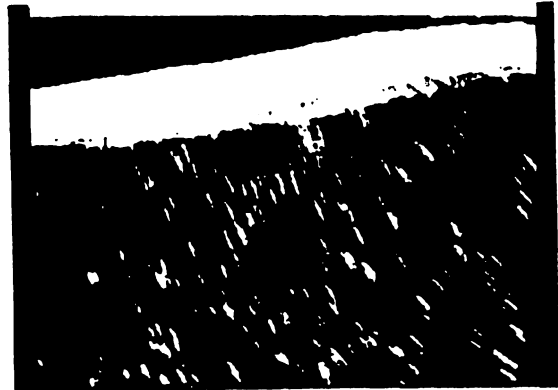


Figure 12 Single binary image of a streak line sequence.